**DE GRUYTER** Open Chemistry 2024; 22: 20240077

**Research Article**

Deepak Singh Panwar, Ram Chandra Chaurasia, Bhupendra Singh Ken, Balraj Krishnan Tudu, Vishal Shah, Jigesh Mehta, Abhinav Kumar, Mushtaq Ahmad Ansari, Lakshmaiya Natrayan, Ishfaq Ahmed Malik*

# Effect of transition metal chloride ($ZnCl_2$) on low-temperature pyrolysis of high ash bituminous coal

https://doi.org/10.1515/chem-2024-0077
received May 11, 2024; accepted July 24, 2024

**Abstract:** Concerns about pollution and global warming have grown in recent years. Efficient coal use is critical for reducing the environmental toll of fossil fuel consumption. This study aims to examine how transition metal chlorides affect the burn-off rate and thermal conversion efficiency of bituminous coal with a high ash content. The analytical methods used include proximate, thermo-gravimetric, morphological, and pyrolysis analyses. This research examined the effect of change in the carbonization temperature, carbonization time, and catalyst concentration on the thermal degradation of high-ash bituminous coal impregnated with $ZnCl_2$. At various ratios, zinc chloride solution was adsorbed onto the coal surface. The treated coal was then heated at different temperatures ranging from 510 to 710°C, under atmospheric pressure, in a furnace without air. This process was carried out to enhance the rate of burnout or pyrolysis. The response surface approach reveals that the carbonization time is a crucial input parameter, followed by the carbonization temperature and catalyst concentration. The response surface methodology analysis yielded a coefficient of determination of 0.9734.

**Keywords:** thermal conversion, high ash bituminous coal, low-temperature pyrolysis, impregnation, response surface methodology

## 1 Introduction

Coal is the predominant source of energy generation in several nations, even in the present day. The need for coal is rising due to the intricacy of using other energy sources such as petroleum, gaseous fuels, and nuclear power. The release of substantial $CO_2$ and other greenhouse gases is a significant environmental concern associated with using fossil fuels [1]. Catalytic pyrolysis of coal leads to the formation of char, which has a large surface area and exhibits significant reactivity toward oxidizing gases. Additionally, this process reduces the fluidity of coal at high temperatures and increases its molecular weight. Coal pyrolysis and gasification yield both gaseous and liquid fuels; however, it requires significant investment due to the requirement for complex and costly equipment to reach high temperatures [2–13]. Like the direct burning of solid fuel, the "burn off" process demonstrates high reactivity with oxygen, producing gaseous byproducts. Although many studies have used kinetic analysis to support the presence of the "burn-off" response [14–20], detecting this reaction may be difficult for many reasons.

An intriguing component of the issue may be explored by exploring the mechanism of this reaction and how it relates to the oxygen adsorption process. Coal gasification, pyrolysis, and oxidation were facilitated by the abundance of free radicals on coal particle surfaces and in newly formed coal fissures [21,22]. As highlighted by Zhan et al. [23], the level of free radicals plays a crucial role in primarily influencing the "burn-off" response. Coal typically has three types of pores: macro-porous, meso-porous, and micro-porous. These pores have a role in the absorption

---

*** Corresponding author: Ishfaq Ahmed Malik,** Department of Economics, Debre Berhan University, Somali, Ethiopia, e-mail: IshfaqAhmed@dbu.edu.et
**Deepak Singh Panwar, Bhupendra Singh Ken, Balraj Krishnan Tudu, Vishal Shah, Jigesh Mehta:** Department of Chemical Engineering, SOE, P P Savani University, Surat, 394125, India
**Ram Chandra Chaurasia:** Department of Mining and Mineral Processing, LNCT, Jabalpur, 482053, Madhya Pradesh, India
**Abhinav Kumar:** Department of Nuclear and Renewable Energy, Ural Federal University Named After the First President of Russia Boris Yeltsin, 620002 Ekaterinburg, Russia
**Mushtaq Ahmad Ansari:** Department of Pharmacology and Toxicology, College of Pharmacy, King Saud University, Riyadh 11451, Saudi Arabia
**Lakshmaiya Natrayan:** Department of Mechanical Engineering, Saveetha School of Engineering, SIMATS, Chennai, Tamil Nadu, India

and adsorption of fluids on the surface of coal [24,25]. Zinc chloride ($ZnCl_2$) and tin chloride ($SnCl_2$) are effective Lewis acids for activating carbonaceous materials like coal. When these acids are dissolved in a liquid and come into contact with coal, they are absorbed onto the surface and into the coal. Prior research indicates that Lewis acids enhance the production of char and gaseous byproducts while reducing the development of tar [26–28]. When coal is treated with Lewis acids and heated without air or oxygen, it undergoes gasification, resulting in the liberation of gaseous products and decreased weight/mass [8,27,29]. The primary determinant of the gasification or combustion rate is the rate of weight loss over time [30,31].

Determining how different process variables affect the process's reaction has recently become possible using multivariate statistical tools. An experimental design is used to study the main and combined impacts of process variables using a small number of experiments. One statistical method that may be used to construct functional linkages between dependent and independent variables is response surface methodology (RSM).

Coal is an essential and crucial energy source on a global scale, particularly in regions that have substantial coal reserves and well-established coal-fired power infrastructure. Nevertheless, the burning of high-ash bituminous (HAB) coal is inherently restricted, which hampers its efficient use and adds to environmental harm. The novelty of this research is to gather information on the effect and mechanism of transition metals on improving the heat release efficiency of coal pyrolysis. Catalytic experiments often use $ZnCl_2$, a low-cost transition metal chloride. Thermal analyses select $ZnCl_2$ to explore its effects on the "burn-off" reaction and heat release of HAB coal. However, very few scholars have focused on the effect and mechanism of transition metals on improving the heat release efficiency of coal pyrolysis. Thermal analyses (TG-DSC), proximate analysis, FESEM, and EDX analyses specifically discuss the mechanism and key factor of the pyrolysis reaction, potentially offering a new approach to the efficient use of HAB materials. The effect of carbonization temperature, carbonization time, and catalyst ($ZnCl_2$) concentration was analyzed utilizing RSM.

## 2 Materials and methods

**Table 1:** Proximate and ultimate analyses of HAB coal sample

| Proximate analysis (%) | | Ultimate analysis (%) | |
|---|---|---|---|
| Moisture | 0.56 | Carbon | 37.92 |
| VM | 13.12 | Hydrogen | 1.79 |
| Ash | 52.53 | Nitrogen | 1.46 |
| FC | 33.79 | Sulfur | 0.62 |
| GCV (cal/g) | 3631.00 | Ash | 52.53 |
| | | Oxygen | 5.68 |

An HAB coal sample was supplied by Geocoal Engineering Private Limited (Dhanbad district, India). The collected coal sample was processed by various methods to meet our desired size (1.5 mm) for analysis. The feed sample utilized for catalytic decomposition is analyzed in both proximate and ultimate analyses, as shown in Table 1. The methods involve making $ZnCl_2$ solutions with varying mass percentages (3, 6, and 9%). Then, this solution is poured into the 10 g coal sample in the beaker and left for some time (30 min) so that $ZnCl_2$ can adequately adsorb on the coal. The coal sample was dried in an air drier set at 100 ± 10°C after 30 min to eliminate any water absorbed onto the coal's surface. Coal samples of known mass are placed in a silica crucible and placed in a close-mouth muffle furnace maintained at three different temperatures: 510, 610, and 710°C. To determine burn-off%, the crucible is taken out after 10, 20, and 30 min, and weight loss is measured with respect to time given for burn-off%.

Instantaneous reactivity ($R_t$) at different reaction times is calculated from the following equation:

$$R_t = (1/W_t) \times (\mathrm{d}w/\mathrm{d}t), \tag{1}$$

where $W_t$ is the weight of the unreacted char and the ($\mathrm{d}w/\mathrm{d}t$) slope of the burn-off vs time $t$, respectively.

### 2.1 Proximate analysis

Following the method outlined by the Bureau of Indian Standards, proximate analysis was carried out [32]. Coal with a particle size of −212 μm was produced to carry out the analysis. Then, coal ash content, moisture, and volatile matter (VM) were measured using 1 g of coal for each study.

### 2.2 Thermo-gravimetric analysis (TGA)

TGA tests were conducted using the Mettler Toledo and Netzsch equipment at the CSIR-CSMCRI facility in Bhavnagar. A 10 mg coal sample in powdered form was heated at 10°C per minute in the presence of nitrogen gas until it reached a temperature of 1,000°C.

### 2.3 Morphological analysis

To determine if the surface morphology of the coal particles changed after $ZnCl_2$ treatment, FE-SEM and EDX analyses were performed. A platinum-coated evacuated die was used to compress −212 μm samples of HAB coal into conductive pellets. The pellets were examined using an airtight chamber and a JEOL JSM 7100F at CSIR-CSMCRI, Bhavnagar.

### 2.4 Pyrolysis analysis

Precise amounts of HAB coal samples and impregnated coal samples were weighed in silica crucibles. These crucibles were placed in a sealed Muffle furnace at 510, 610, and 710°C. During the burn-off process, the crucible was removed after 10 min, and the weight lost was determined to calculate the percentage of burn-off over time. This process is iterated until the weight is consistently measured.

### 2.5 RSM

The Box–Behnken design (BBD) is a popular statistical experimental design in RSM [33]. Modeling, experiment design, and workflow optimization are all made easier by RSM, a collection of statistical and mathematical tools. When looking at the impact of several factors on a response, the BBD is a great tool. Due to its factorial nature, the BBD allows the simultaneous manipulation of several parameters to ascertain their influence on the final outcome. To conduct a more comprehensive analysis of the variable, this technique often incorporates three levels of each component: low, middle, and high. The BBD is believed to be efficient when evaluating the amount of trials required to get precise data on the components and their interactions. The primary goal of the BBD is to create a mathematical model that translates the input feed components into a response variable. Researchers may use it to analyze experimental data using analysis of variance (ANOVA), which helps identify key factors and interactions. The BBD is widely used by researchers to optimize processes with many variables in many fields, including medicine, chemistry, engineering, and manufacturing.

The association between the variables was established using a best-fitting second-order polynomial equation. The equation based on the fitted model is as follows:

$$y = \beta_0 + \sum_{i=1}^{k} \beta_i x_i + \sum_{j=1}^{k} \beta_{jj} x_j^2 + \sum\sum_{ij}^{k} \beta_{ij} x_i x_j + \varepsilon, \quad (2)$$

where $Y$ is the predicted response, $\beta_0$ is a constant, and the coefficients for linear, interaction, and quadratic effects are represented by $\beta_i$, $\beta_{ij}$, and $\beta_{jj}$, respectively. In the equation, $\varepsilon$ represents the residual. Our ANOVA was used to determine the model's significance, with a confidence level of $\alpha = 0.05$. The lack of fit, $F$- and $p$-values are some of the methods employed by statisticians to determine the relative importance of each parameter. The experiment design, statistical analysis, and response surface studies were all conducted using Design-Expert 13.

## 3 Results and discussion

### 3.1 Structure characteristics of $ZnCl_2$-loaded HAB coal samples

SEM imaging was used to identify changes in the surface morphology of coal particles after $ZnCl_2$ treatment. This method may involve differences in the particle size, shape, and surface roughness relative to untreated coal particles. HAB coal samples were activated using the salt impregnation method to analyze the catalytic effects of $ZnCl_2$ salts on the surface of HAB coal during combustion and gasification. Under the treatment of $ZnCl_2$ salts in an aqueous solution, fragments and various sizes of holes occur on the surface of HAB coal, while the reaction of $ZnCl_2$ salts on coal mainly results in the creation of tiny fragments. These findings indicate the depolymerization or rebuilding of coal surface structure after $ZnCl_2$ salt impregnation. $ZnCl_2$ loading could lead to agglomeration, which results in the development of more extensive clusters or aggregates of coal particles. The existence of pits, fissures, or protrusions on the coal particle surface could influence surface reactivity and interaction with other components during combustion or gasification processes. The SEM images of HAB coal and Zn-loading samples are shown in Figure 1.

### 3.2 Thermogravimetric (TG)-Differential thermogravimetric (DTG) analysis of $ZnCl_2$-loaded HAB coal samples

Figure 2(a) and (b) displays the thermal analysis curves of TG-DTG for the untreated and $ZnCl_2$-treated coal samples. The TGA curve shown in Figure 2(a) demonstrates slight fluctuations in weight loss in the temperature range of

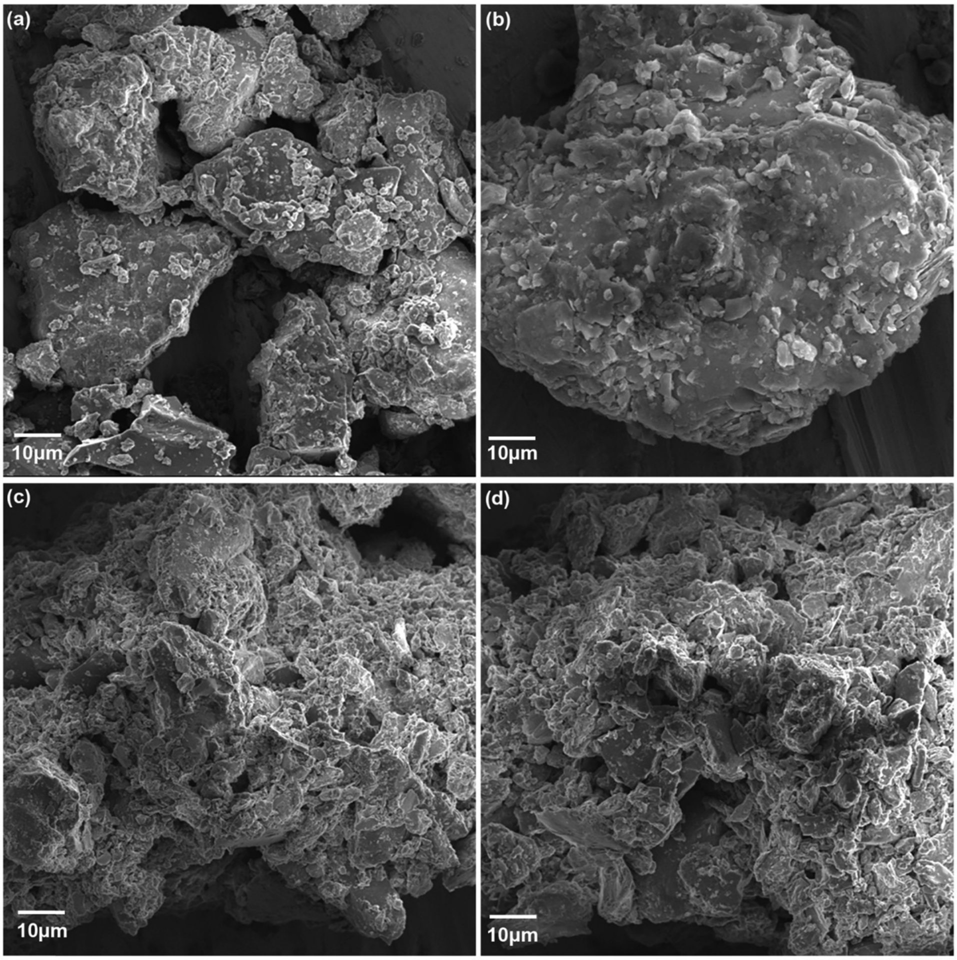

**Figure 1:** SEM micrographs of raw and impregnated coal samples: (a) coal, (b) coal–3%_$ZnCl_2$, (c) coal–6%_$ZnCl_2$, and (d) coal–9%_$ZnCl_2$.

25–160°C, suggesting a low level of moisture. In addition, the process of weight loss caused by the production of VM starts after reaching a temperature of 350°C for all the samples. The pyrolysis process is initiated after reaching a temperature of 480°C, resulting in a significant and fast reduction in weight. Once the temperature reaches 600°C, the coal samples experience a minimal decrease in weight, indicating that no more substances are available for combustion and that the pyrolysis process has concluded. The delay in pyrolysis is due to the sample's elevated burnout temperature and diminished porous structure [34].

The temperatures that define specific properties, such as the temperature at which ignition occurs ($T_i$), peak temperature ($T_p$), and burnout temperature ($T_f$) during the pyrolysis process, may be identified using DTG analysis, as shown in Figure 2(b). The pyrolysis behavior of raw coal and $ZnCl_2$-treated samples requires a thorough understanding of these characteristics. An evident disparity in the pyrolysis profile is seen between the raw sample and those with varying concentrations of $ZnCl_2$, namely 3, 6, and 9%. Based on the information shown in Figure 2(b), it can be deduced that the raw coal to 9% $ZnCl_2$ samples have a lower ignition temperature, namely approximately 395–380°C. Nevertheless, there is a decrease in the ignition temperature ($T_i$) as the concentration of $ZnCl_2$ increases, ranging from 3 to 9%. The change observed may be related to the increased prevalence of VM release in $ZnCl_2$ samples with lower concentrations (3, 6, and 9%). This facilitates the coal samples' pyrolysis and combustion process. A solitary peak in all samples suggests a step-by-step and uninterrupted decomposition process characterized by the elimination of water and the depletion of complex hydrocarbon compounds from the sample [35]. The burnout temperatures for all samples fall within the range of 511–720°C. Nevertheless, a higher concentration of $ZnCl_2$ leads to an elevation in the burnout temperature, causing a decrease in the pyrolysis rate and increasing the time needed for the pyrolysis process to be fully completed [34–38].

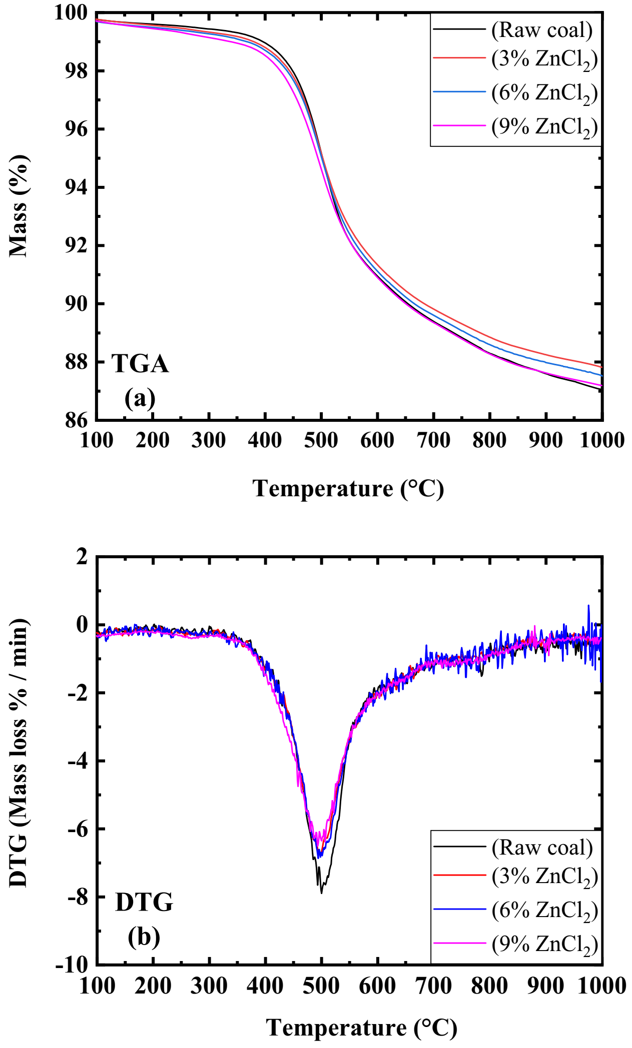

**Figure 2:** (a) TGA of raw coal and different $ZnCl_2$-treated samples. (b) DTG of raw coal and different $ZnCl_2$-treated samples.

## 3.3 Kinetic analysis of $ZnCl_2$-loaded HAB coal samples

The Coats–Redfern (C–R) method was used for kinetic analysis, but other models were not considered. The C–R method [36] is a first-order reaction with an integral rate equation mainly used for the calculation of activation energy ($E$) and pyrolysis kinetic parameters like the pre-exponential factor ($A$) and regression coefficient ($R^2$), compared to other methods. In this method, $E$ is calculated from the linearized plot pyrolysis data attained through TGA as $\ln\frac{-\ln(1-x)}{T^2}$ vs $1/T$ from equation (1) [36] as follows:

$$\ln\frac{-\ln(1-x)}{T^2} = \ln\left(\frac{AR}{HE}\left[1 - \left(\frac{2RT}{E}\right)\right]\right) - \frac{E}{RT}, \qquad (3)$$

where $x$ is the proportion of coal that is burnt at a certain time $t$, $n$ is the order of the pyrolysis process, $H$ is the heating rate in °C/min, $E$ is the activation energy of coal in kJ/mol, $A$ is the frequency factor in $\text{min}^{-1}$, $T$ is the temperature in K, and $R$ is the universal gas constant (= 8.314 J/K mol).

Table 2 demonstrates a negative correlation between the pyrolysis efficiency ($E$) and the concentration of $ZnCl_2$, indicating that as the concentration of $ZnCl_2$ increases, the pyrolysis efficiency decreases. Similarly, a decrease was seen in the value of $A$ from 26.19 to 4.16 per minute. The activation energy ($E$) decreases from 42.91 to 31.92 kJ/mol. The decrease in noncombustible material in the porous structure of coal is responsible for this drop. The activation energy decreases more. The pyrolysis process can explain this trend, which generates numerous active sites within the coal structure. These active sites facilitate easier and smoother pyrolysis, leading to decreased activation energy [34–38].

## 3.4 Effect of carbonization time on HAB coal samples

This work indicates that impregnated coal becomes more reactive as carbonization time increases. Up to 30 min at 510°C, there was a significant increase in weight loss, but the change in reactivity slowed beyond that point. Coal's reactivity increases with carbonization time at a constant temperature. The carbonization temperature of 610°C resulted in a significant increase up to 30 min, followed by a steady weight decrease. A similar trend was seen at 710°C, as shown in Figure 3(a)–(c). Weight loss was lower at

**Table 2:** Pyrolysis characteristic profile and kinetic analysis of raw and treated coal samples

| Sample no. | $T_i$ (°C) | $T_p$ (°C) | $T_f$ (°C) | $DTG_{max}$ (%/min) | Mass loss (%) | $R^2$ | $A$ ($\text{min}^{-1}$) | $E$ (kJ/mol) |
|---|---|---|---|---|---|---|---|---|
| Raw coal | 393.88 | 511.87 | 718.89 | −7.42 | 12.51 | 0.899 | 26.1965 | 42.9152 |
| 3% $ZnCl_2$ | 388.16 | 499.17 | 719.17 | −6.736 | 12.22 | 0.922 | 18.3237 | 40.3986 |
| 6% $ZnCl_2$ | 386.93 | 493.93 | 719.93 | −6.865 | 12.09 | 0.922 | 15.2531 | 39.2945 |
| 9% $ZnCl_2$ | 384.05 | 493.20 | 782.00 | −6.501 | 11.50 | 0.897 | 4.16582 | 31.9258 |

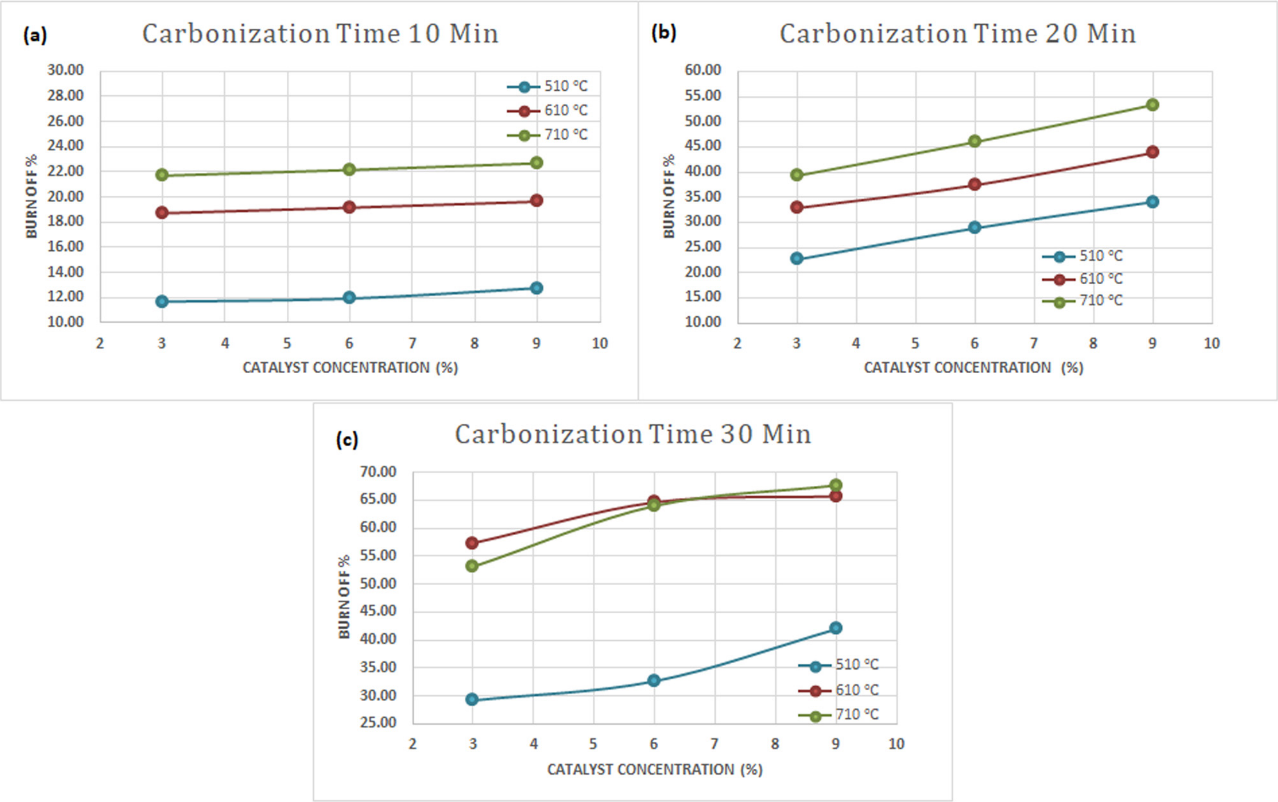

**Figure 3:** Effect of (a) carbonization temperature with change in the catalyst concentration at 10 min, (b) carbonization temperature with change in the catalyst concentration at 20 min, and (c) carbonization temperature with change in the catalyst concentration at 30 min.

510°C compared to that at 610 and 710°C. Reducing surface area and micropore volume caused by carbon shrinkage at higher temperatures leads to significant weight loss in HAB coal.

## 3.5 Effect of $ZnCl_2$ concentration on HAB coal samples

It was observed in many studies that $ZnCl_2$ concentration significantly affects the pyrolysis, combustion, and gasification process. Figure 4(a)–(c) demonstrates that $ZnCl_2$ concentration significantly affects burn-off%. Increasing $ZnCl_2$ concentration leads to a considerable increase in burn-off of up to 9% and significantly decreases at a constant temperature and carbonization time at lower concentrations. Many researchers reported similar results [26,39]. The highest reduction was achieved with 9% $ZnCl_2$-impregnated coal at 610 and 710°C.

## 3.6 Effect of carbonization temperature on HAB coal samples

The effect of carbonization temperature on HAB coal is shown in Figure 5(a)–(c), which illustrates that increasing the carbonization temperature leads to increased weight loss at the same catalyst concentration and time. Higher temperatures may shift the coal particle porosity from micro-porosity to macro-porosity, as shown in previous studies [40,41]. Gases (VM) evolve faster at higher temperatures of 710°C than at lower temperatures of 510°C.

## 3.7 RSM

In the present study, three process variables were varied: carbonization time, catalyst concentration, and carbonization temperature; the results are tabulated. The coded and uncoded levels of the process variables are shown in Table 3.

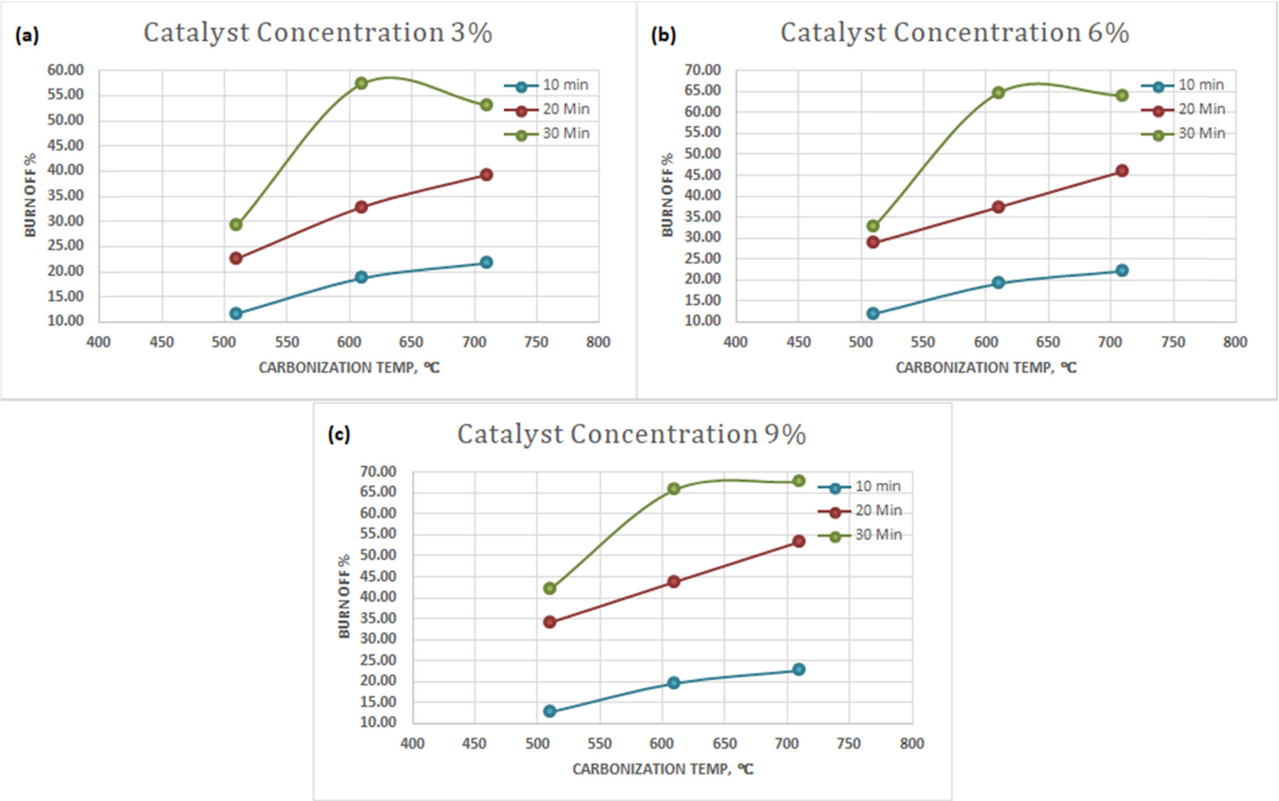

**Figure 4:** Effect of (a) concentration-time with the change in the concentration temperature at 3%, (b) concentration-time with the change in the concentration temperature at 6%, and (c) concentration-time with the change in the concentration temperature at 9%.

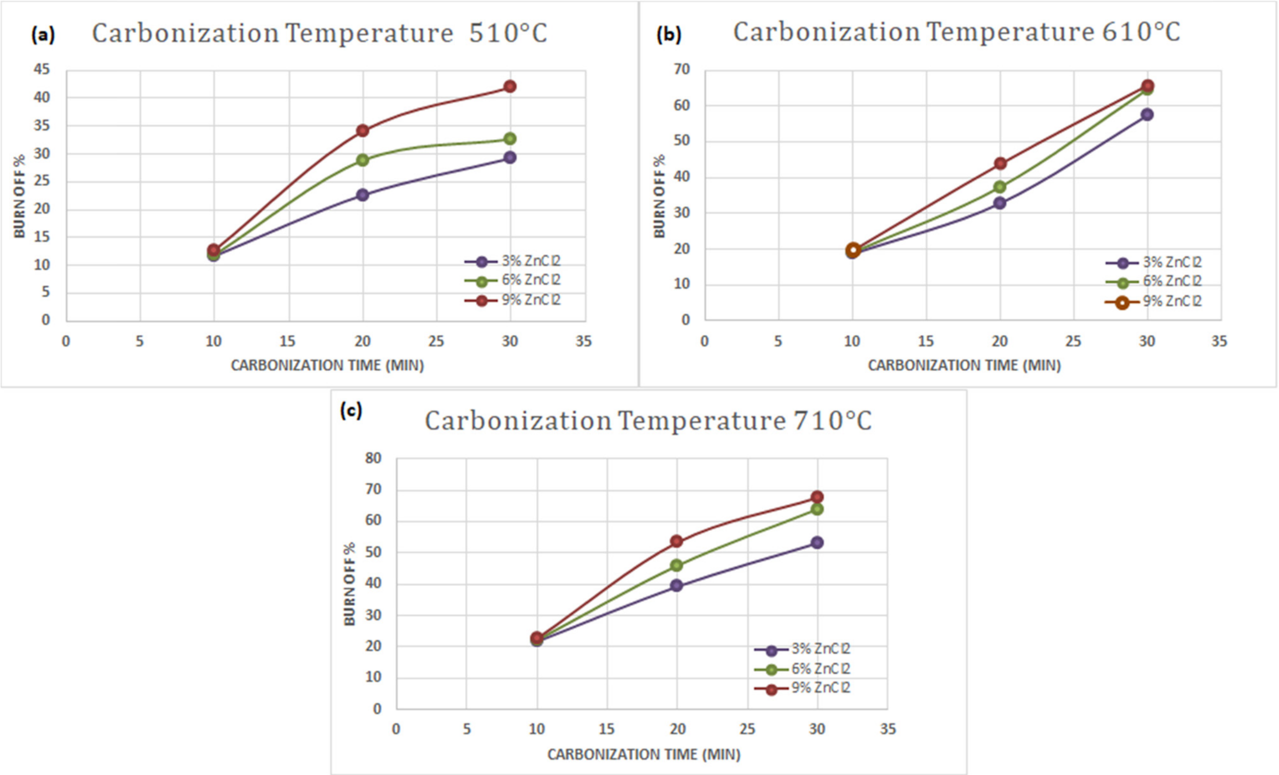

**Figure 5:** Effect of (a) catalyst concentration with change in time at 510°C, (b) catalyst concentration with change in time at 610°C, and (c) catalyst concentration with change in time at 710°C.

**Table 3:** Coded and uncoded levels of variables for the BBD

| Variables | Coded symbol | Levels and range | | |
|---|---|---|---|---|
| | | −1 | 0 | 1 |
| Carbonization time (min) | A | 10 | 20 | 30 |
| Catalyst concentration (%) | B | 3 | 6 | 9 |
| Carbonization temperature (°C) | C | 510 | 610 | 710 |

A BBD of 15 experiments for studying the effect of three variables on burn-off rate: carbonization time (A), catalyst concentration (B), and carbonization temperature (C), as shown in Table 4.

The different combinations of variables resulted in burn-off% varying between 11.93 and 67.68%. The predicted values using the model given by the BBD ranged between 10.17 and 74.51%. From the data presented, a relationship between the response and process variables was attained and expressed in a second-order quadratic equation as follows:

$$\begin{aligned}\mathrm{BO}(\%) = 38 + 18.11A + 3.92B + 9.69C - 1.45A^2 + 3.19B^2 \\ - 3.86C^2 + 0.9775AB + 5.28AC + 0.655BC.\end{aligned} \tag{4}$$

Results from the ANOVA are shown in Table 5, confirming the model's statistical significance.

Predicting the percentage of burn-off, the model's forecast was considered significant with a $p$-value of less than 0.001. With an $R^2$ value of 0.9734, we may conclude that the experimental variables under consideration account for all of the variation in burn-off%. The model is very relevant when the modified $R^2$ value is close to the $R^2$ coefficient. If the sign of the coefficient is positive, then the variables have an additive impact on the burn-off%. If it is negative, then the variables have an antagonistic effect. Statistical analysis revealed that there were positive linear effects of carbonization time ($p < 0.000$), catalyst concentration ($p < 0.057$), and carbonization temperature ($p < 0.001$) on the sample.

**Table 4:** BBD matrix showing observed response and predicted response

| C. Time | Cat. Conc. | C. Temp. | Observed % BO | Predicted % BO |
|---|---|---|---|---|
| −1 | −1 | 0 | 18.71 | 18.69 |
| 1 | −1 | 0 | 57.88 | 52.95 |
| −1 | 1 | 0 | 19.64 | 24.57 |
| 1 | 1 | 0 | 62.72 | 62.75 |
| −1 | 0 | −1 | 11.93 | 10.17 |
| 1 | 0 | −1 | 32.67 | 35.83 |
| −1 | 0 | 1 | 22.15 | 18.99 |
| 1 | 0 | 1 | 64.02 | 65.77 |
| 0 | −1 | −1 | 22.61 | 24.38 |
| 0 | 1 | −1 | 34.08 | 30.91 |
| 0 | −1 | 1 | 39.27 | 42.45 |
| 0 | 1 | 1 | 53.36 | 51.60 |
| 0 | 0 | 0 | 37.4 | 38.00 |
| 0 | 0 | 0 | 38.1 | 38.00 |
| 0 | 0 | 0 | 38.5 | 38.00 |

**Table 5:** ANOVA table of the quadratic model for the catalytic thermal conversion of coal

| Source | DF | Seq SS | Adj MS | *F*-value | *P*-value |
|---|---|---|---|---|---|
| Model | 9 | 3721.25 | 413.47 | 20.32 | 0.002 |
| A-Carbonization time | 1 | 2623.05 | 2623.05 | 128.89 | <0.0001 |
| B-Catalyst concentration | 1 | 122.7 | 122.7 | 6.03 | 0.0576 |
| C-Carbonization temperature | 1 | 750.98 | 750.98 | 36.9 | 0.0017 |
| $A^2$ | 1 | 7.76 | 7.76 | 0.3815 | 0.5639 |
| $B^2$ | 1 | 37.51 | 37.51 | 1.84 | 0.2326 |
| $C^2$ | 1 | 54.94 | 54.94 | 2.7 | 0.1613 |
| AB | 1 | 3.82 | 3.82 | 0.1878 | 0.6828 |
| AC | 1 | 111.62 | 111.62 | 5.48 | 0.0662 |
| BC | 1 | 1.72 | 1.72 | 0.0843 | 0.7832 |
| Residual | 5 | 101.75 | 20.35 | | |
| Lack of fit | 3 | 101.13 | 33.71 | 108.75 | 0.0091 |
| Pure error | 2 | 0.62 | 0.31 | | |
| Total | 14 | 3823.01 | | | |

$R^2 = 0.9734$.

On the other hand, as their $p$-values were more than 0.05, the quadratic terms of carbonization time ($p < 0.563$), catalyst concentration ($p < 0.232$), and carbonization temperature ($p < 0.161$) were determined to be non-significant. The statistical significance of the interaction effects between concentration and time ($p < 0.0682$), time and temperature ($p < 0.066$), and concentration and temperature ($p < 0.783$) is shown to be insignificant. A $p$-value < 0.002 and an $F$-value of 20.32 characterize the quadratic model. The strong $F$-values demonstrate the model is statistically significant [33,42,43]. The carbonization time is the most important process element, contributing 68.61% of the total, followed by the catalyst concentration at 3.20% and the carbonization temperature at 19.64%. Accordingly, carbonization time is the most important factor, followed by carbonization temperature and catalyst concentration, regarding the burn-off hierarchy. A variety of process parameters were examined using the RSM 3D plots.

In RSM plots, two factors are shown to affect the response variable while the remaining variables are held at their intermediate values. Figure 6(a)–(c) shows that the

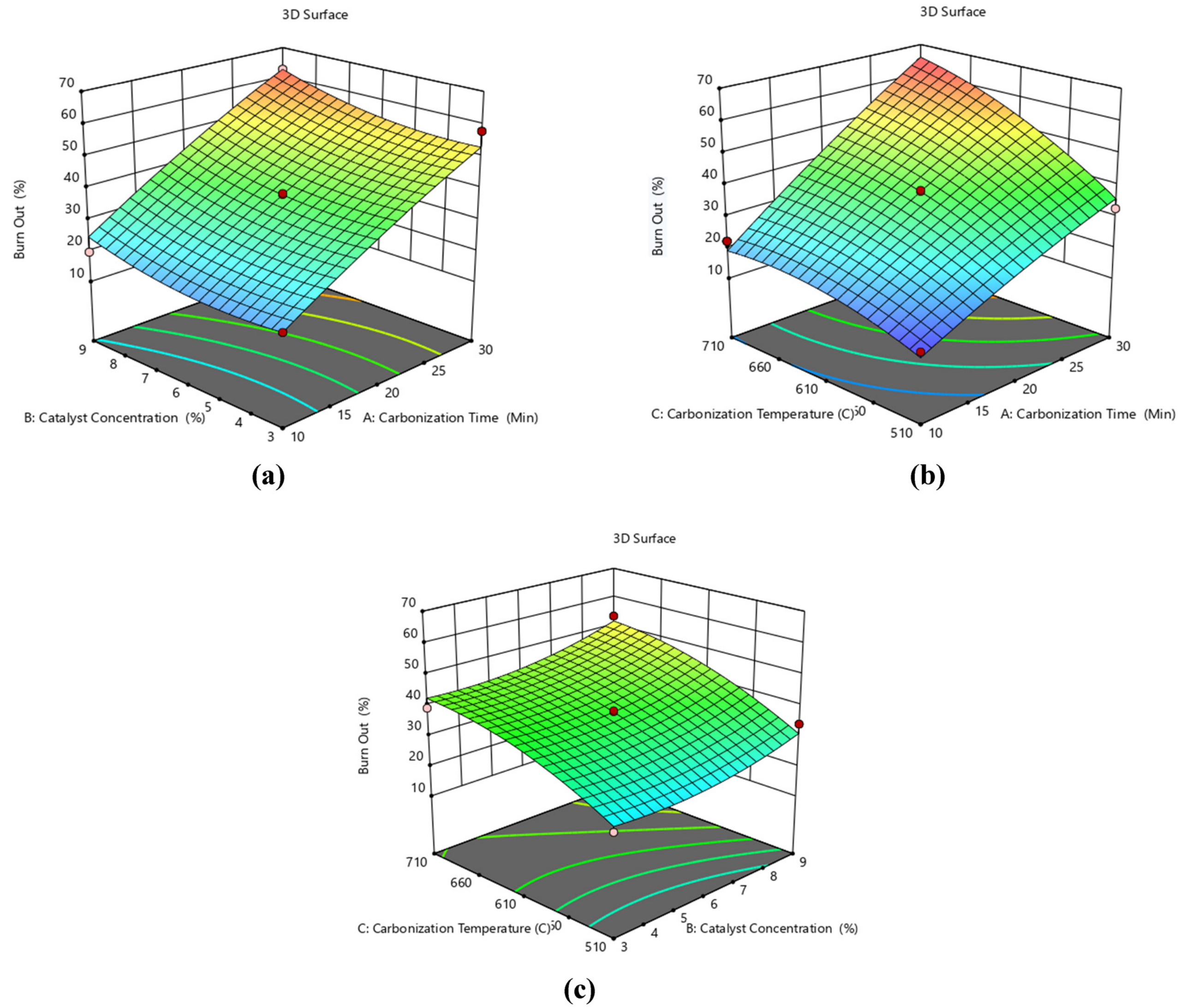

**Figure 6:** Effect of variables on the response in a 3D surface: (a) effect of time and concentration on burn-off%, (b) effect of concentration and temperature on burn-off%, and (c) effect of time and temperature on burn-off%.

pyrolysis rate significantly increases when the carbonization time increases. The optimal pyrolysis rate was seen when the catalyst concentration was low and the carbonization period was high. An analogous pattern of transformation was seen when the carbonization temperature was raised. The pyrolysis rate was greater at elevated temperatures (710°C) for both the concentration and carbonization time. The tight correspondence between the actual and anticipated values, as shown by the substantial $R^2$ value, confirms the importance of the model predicted by the RSM BBD, as shown in Figure 7.

## 4 Conclusions

Although $ZnCl_2$ has been shown to improve the combustion of HAB coal, many unanswered questions and neglected research topics remain. This study focuses on the technical details of adjusting the $ZnCl_2$ dose to ensure equal distribution, long-term stability, and compatibility with current combustion systems. This report lays forth potential avenues for research that might lead to developments in this field. Among them, there is a pressing need for scale-up studies, techno-economic evaluations, and a deeper dive

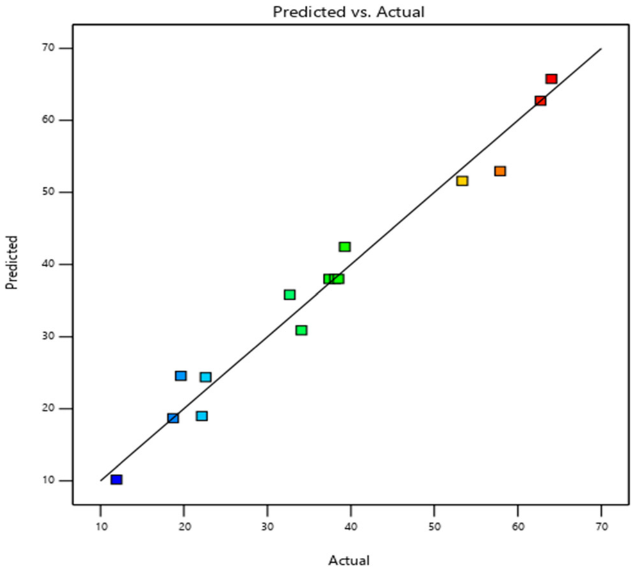

**Figure 7:** Comparison between prediction with observed values for burn-off%.

into the underlying processes. The surface of HAB coal becomes speckled with pieces and holes of varying sizes when treated with a water solution of $ZnCl_2$ salts. Tiny pieces are the main byproduct of the reaction between coal and $ZnCl_2$ salts. Evidence from the data points to depolymerization or rebuilding of the coal surface structure after impregnation with $ZnCl_2$ salt. Adding $ZnCl_2$ can potentially make the coal particles agglomerate or clump together. Using TG-DTG analysis, pyrolysis tests show that HAB coal exhibits improved ignition properties when treated with $ZnCl_2$ concentrations ranging from 3 to 9% compared to untreated coal. The activation energy of the treated coal decreased from 42.91 to 31.92 kJ/mol when treated with 9% $ZnCl_2$, lending credence to this claim. Typically, the ignition temperature ($T_i$) and peak temperature ($T_p$) decrease as one moves from untreated coal to coal treated with 9% $ZnCl_2$. The decrease in ignition temperature (from 393.88 to 384.05°C) and peak temperature (511.87 to 493.20°C) is more apparent. However, there is an increase in the burning temperature of clean coal. The reduced ash content of the coal samples causes the pyrolysis process to go into its later phases. The reduced Ti and Tp levels in the treated coal samples indicate an increase in ignitability, which is beneficial for pyrolysis operations and power plants.

Research on coal pyrolysis properties and the effects of $ZnCl_2$ treatment has concluded that a $ZnCl_2$ concentration of 9% is optimum for mineral removal from HAB coal. Using RSM to predict burn-off percentage is a rigorous approach, and the coefficient of determination ($R^2$) is 0.9734. The quadratic model showed that the predicted values were in agreement with those obtained experimentally. The developed model considered the carbonization time as the primary input, and the carbonization temperature and catalyst concentration were the secondary and most essential input parameters.

**Acknowledgements:** The authors acknowledge and extend their appreciation to the Researchers Supporting Project Number (RSPD2024R996), King Saud University, Riyadh, Saudi Arabia, for funding this study.

**Funding information:** The authors acknowledge and extend their appreciation to the Researchers Supporting Project Number (RSPD2024R996), King Saud University, Riyadh, Saudi Arabia for funding this study.

**Author contributions:** Conceptualization, Methodology, Visualization, Investigation, Writing – Original Draft, Writing – Review & Editing, Project administration – DSP, RCC; Resources Visualization – VS, JM, AK, MAA, IAM, LN; Formal analysis and Investigation – BSK, BKT. All the authors agreed on the final version of the manuscript.

**Conflict of interest:** Authors state no conflict of interest.

**Data availability statement:** The data used to support the findings of this study are available from the corresponding author upon request.

## References

[1] Gad MS, Panchal H, Ağbulut Ü. Waste to Energy: An experimental comparison of burning the waste-derived bio-oils produced by transesterification and pyrolysis methods. Energy. Mar. 2022;242:122945. doi: 10.1016/j.energy.2021.122945.

[2] Patil S, Ramesh B, Sathish T, Saravanan A, Almujibah H, Panchal H, et al. Evaluation and optimization of mechanical properties of laterized concrete containing fly ash and steel fiber using Taguchi robust design method. Alex Eng J. Jan. 2024;87:682–706. doi: 10.1016/j.aej.2023.12.009.

[3] Petit JC. Calorimetric evidence for a dual mechanism in the low temperature oxidation of coal. J Therm Anal Calorim. 1991;37(8):1719–26.

[4] Altuntaş Öztaş N, Yürüm Y. Effect of catalysts on the pyrolysis of Turkish Zonguldak bituminous coal. Energy Fuels. 2000;14(4):820–7.

[5] Chang Z, Chu M, Zhang C, Bai S, Ma L. Investigation of the effect of selected transition metal salts on the pyrolysis of Huadian oil shale, China. Oil Shale. 2017;34(4):354–67.

[6] He Y, Yuan Y, Wang Z, Liu L, Tan J, Chen J, et al. Kinetics and Mechanisms of Metal Chlorides Catalysis for Coal Char Gasification with CO2. Catalysts. 2020;10(6):715.

[7] Ibarra J, Moliner R, Palacios J. Catalytic effects of zinc chloride in the pyrolysis of Spanish high sulphur coals. Fuel. 1991;70(6):727–32.
[8] Jolly R, Charcosset H, Boudou JP, Guet JM. Catalytic effect of ZnCl2 during coal pyrolysis. Fuel Process Technol. 1988;20:51–60.
[9] Li Y, Yang H, Hu J, Wang X, Chen H. Effect of catalysts on the reactivity and structure evolution of char in petroleum coke steam gasification. Fuel. 2014;117:1174–80.
[10] Zhou C, Zhao L, Zheng J, Wang K, Deng H, Liu P, et al. Catalytic effect of metal chlorides on coal pyrolysis and gasification part I. Combined TG-FTIR study for coal pyrolysis. Thermochim Acta. 2017;655:331–6.
[11] Liu L, Yuan Y, Kumar S, Wang Z, He Y, Lv Y, et al. Catalytic effect of metal chlorides on coal pyrolysis and gasification part II. Effects of acid washing on coal characteristics. Thermochim Acta. 2018;666:41–50.
[12] Miyake M, Kagajyo T, Nomura M. Hydrocracking of asphaltene from coal using ZnCl2 as catalyst. Fuel Process Technol. 1984;9(3):293–306.
[13] Nomura M, Sakashita H, Miyake M, Kikkawa S. Comparison of coal hydroliquefaction catalysed by ZnCl2-MCln (CuCl, CrCl3 and MoCl5) and ZnCl2 melts. Fuel. 1983;62(1):73–7.
[14] Wang H, Dlugogorski BZ, Kennedy EM. Kinetic modeling of low-temperature oxidation of coal. Combust Flame. 2002;131(4):452–64.
[15] Wang H, Dlugogorski BZ, Kennedy EM. Coal oxidation at low temperatures: oxygen consumption, oxidation products, reaction mechanism and kinetic modelling. Prog Energy Combust Sci. 2003;29(6):487–513.
[16] Qiao L, Mu X, Deng C, Wang X, Wang Y. Experimental study on catalytic action of intrinsic metals in coal spontaneous combustion. ACS Omega. 2023;8(15):13680–9.
[17] Wang W, Lemaire R, Bensakhria A, Luart D. Review on the catalytic effects of alkali and alkaline earth metals (AAEMs) including sodium, potassium, calcium and magnesium on the pyrolysis of lignocellulosic biomass and on the co-pyrolysis of coal with biomass. J Anal Appl Pyrolysis. 2022;163:105479.
[18] Wang Z, Tan J, He Y, Yuan Y, Liu L, Zhu Y, et al. Catalytic effect of metal chloride additives on the volatile gas release characteristics for high-temperature lignite pyrolysis. Energy Fuels. 2019;33(10):9437–45.
[19] Zou X, Yao J, Yang X, Song W, Lin W. Catalytic effects of metal chlorides on the pyrolysis of lignite. Energy Fuels. 2007;21(2):619–24.
[20] Zubek K, Czerski G, Porada S. Determination of optimal temperature and amount of catalysts based on alkali and alkaline earth metals for steam gasification process of bituminous coal. Thermochim Acta. 2018;665:60–9.
[21] Ruthstein S, Cohen H. The involvement of carbon-centered radicals in the aging process of coals under atmospheric conditions: An EPR study. Phys Chem Chem Phys. 2018;20(42):27025–35.
[22] Wu D, Song Z, Schmidt M, Zhang Q, Qian X. Theoretical and numerical study on ignition behaviour of coal dust layers on a hot surface with corrected kinetic parameters. J Hazard Mater. 2019;368:156–62.
[23] Zhan J, Wang H, Zhu F, Song S. Analysis on the governing reactions in coal oxidation at temperatures up to 400 C. Int J Clean Coal Energy. 2014;3(2):19–28.
[24] Bansal RC, Bonnet JB, Stoeckli F. Active Carbon. New York: Marcel Dekker; 1988. p. 1.
[25] Smisek M, Cerny S. Active Carbon: Manufacture, Properties And Applications. Amsterdam: Elsevier Publishing Company; 1970. p. 12.
[26] Ahmadpour A, Do DD. The preparation of active carbons from coal by chemical and physical activation. Carbon. 1996;34(4):471–9.
[27] Kandiyoti R, Lazaridis JI, Dyrvold B, Weerasinghe CR. Pyrolysis of a ZnCI2-impregnated coal in an inert atmosphere. Fuel. 1984;63(11):1583–7.
[28] Shibaoka M, Russell NJ, Bodily DM. Coal Liquefaction model: Microscopic examination of solids from metal halide catalysed coal hydrogenation experiments. Fuel. 1982;61(2):201–3.
[29] Boudou JP, Gérard I, Bégin D, Marêché JF, Furdin G, Albiniak A, et al. Effect of MoCl5 addition on the carbonization and the subsequent steam activation of pitch and coking coals. Carbon. 2000;38(4):525–34.
[30] Parra J, de Sousa J, Pis J, Pajares JA, Bansal RC. Effect of gasification on the porous characteristics of activated carbons from a semi-anthracite. Carbon. 1995;33(6):801–7.
[31] Rodriguez-Reinoso F, Molina-Sabio M. Activated carbons from lignocellulosic materials by chemical and/or physical activation: an overview. Carbon. 1992;30(7):1111–8.
[32] IS 1350 (Part I), Indian standard methods of test for coal and coke, part I: Proximate analysis. New Delhi: Bureau of Indian Standards; 2003. p. 1–28. 2nd Revision.
[33] Chaurasia RC, Sahu D, Nikkam S. Cleaning of coal by multi gravity separator. Trans Indian Inst Met. 2018;71:1487–95.
[34] Ken BS, Nandi BK. Effect of some operational parameters on desulphurization of high sulphur Indian coal by KOH leaching. Energy Explor Exploit. 2018;36(6):1674–91.
[35] Ken BS, Aich S, Saxena VK, Nandi BK. Combustion behavior of KOH desulphurized coals assessed by TGA-DTG. Energy Sources, Part A. 2018;40(20):2458–66.
[36] Gürses A, Doymuş K, Doğar Ç, Yalçin M. Investigation of agglomeration rates of two Turkish lignites. Energy Convers Manag. 2003;44(8):1247–57.
[37] Ken BS, Nandi BK. Cleaning of high sulfur Indian coal by oil agglomeration and leaching. Energy Sources, Part A. 2018;40(9):1027–34.
[38] Ken BS, Nandi BK. Desulfurization of high sulfur Indian coal by oil agglomeration using Linseed oil. Powder Technol. 2019;342:690–7.
[39] Ruiz Bevia F, Prats Rico D, Gomis AFM. Activated carbon from almond shells. Chemical activation. 1. Activating reagent selection and variables influence. Ind Eng Chem product Res Dev. 1984;23(2):266–9.
[40] González-Vilchez P, Linares-Solano A, de D. López-González J, Rodríguez-Reinoso F. The controlled reaction of active carbons with air at 350 C–I: Reactivity and changes in surface area. Carbon. 1979;17(6):441–6.
[41] Rodriguez-Reinoso F, Linares-Solano A, Martín-Martinez JM, López-González JD. The controlled reaction of active carbons with air at 350° C–II: Evolution of microporosity. Carbon. 1984;22(2):123–30.
[42] Chaurasia RC, Nikkam S. Beneficiation of low-grade iron ore fines by multi-gravity separator (MGS) using optimization studies. Part Sci Technol. 2017;35(1):45–53.
[43] Chaurasia RC, Nikkam S. Optimization studies on a multi-gravity separator treating ultrafine coal. Int J Coal Prep Util. 2017;37(4):195–212.